IMPLEMENTATION OF LAND SURFACE BOUNDARY CONDITIONS IN TOUGH2

Stephen W. Webb and James M. Phelan

Sandia National Laboratories
Dangerous Materials Mitigation and Disposition
Albuquerque, NM, 87185-0719, USA
e-mail: swwebb@sandia.gov

ABSTRACT

The land surface is a common boundary for many subsurface problems of interest. The effect of weather conditions and the boundary layer resistance between the soil surface and the weather conditions is very important for the prediction of shallow subsurface conditions. Weather data can be easily obtained worldwide, but some information is often missing. These data are linked to the surface conditions through boundary layers. In the present implementation, a boundary layer profile methodology is described. The resulting surface boundary conditions and boundary layer thickness have significant diurnal variations that may have a significant impact on near-surface behavior.

INTRODUCTION

The land surface is a common boundary for many subsurface problems of interest. The effect of weather conditions and the boundary layer resistance between the soil surface and the weather conditions is very important for the prediction of shallow subsurface conditions. Unlike many boundary conditions for porous media codes like TOUGH2, these parameters (weather and boundary layer behavior) are highly transient and must be properly accounted for in any near-surface analysis.

The application of interest in the present discussion is chemical movement from buried landmines. Because landmines are often only buried a few cm below the soil surface, weather conditions and boundary layer behavior play a dominant role in the transport of landmine chemicals in the soil and to the surface where they can be detected. Webb et al. (1998, 1999) created another variation of the TOUGH2 code named T2TNT for modeling transport in the shallow subsurface with land surface boundary conditions and other modifications to predict landmine chemical signatures (Webb and Phelan, 2000, 2002, 2003, Phelan and Webb, 2003).

ENVIRONMENTAL FACTORS

Figure 1 depicts the principal environmental conditions at the ground surface. Wind has a direct effect on the movement of water vapor from the soil into the atmosphere. Thermal radiation, which consists of solar and long-wave components, impacts the surface and subsurface temperature. The atmospheric conditions (pressure, temperature, and relative humidity) affect gas phase transport to the surface, the surface temperature, and water evaporation from the soil into the atmosphere. Precipitation and runoff directly influence soil moisture. Finally, plant growth and transpiration impact the net transport of radiation to the soil surface, the net water infiltration into the soil, the air-atmosphere transition region, and act as sinks for subsurface water. The effect of plants is not discussed in this paper, not because the effect is unimportant, but because the effect hasn't been included in work to date.

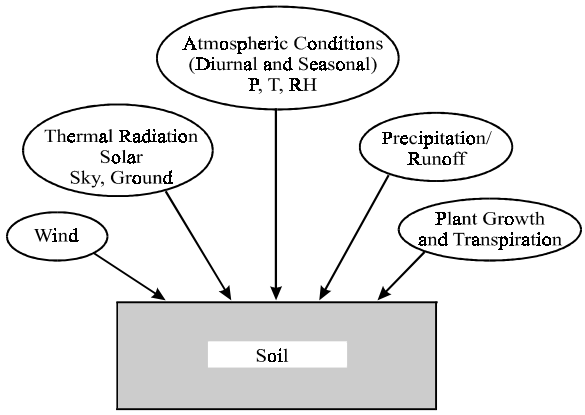

Figure 1. Environmental Factors at the Soil-Atmosphere Interface

The soil-atmosphere interface is a region where heat, wind and vapor transitions occur, which can be described by boundary layers. These boundary layers are often prescribed by steady-state non-linear profiles of temperature, velocity, and concentration that depend on various conditions. This approach is a relatively simple method. Other processes involve more complex phenomena, such as eddy diffusion or localized packet emissions, and require sophisticated computational fluid dynamics approaches.

The T2TNT code uses the boundary layer profile methodology to represent the soil-atmosphere

interface. The model considers water evaporation where the boundary layer is generally a thin (~1-10 cm) layer of air at the soil surface where the water vapor concentration changes from the value at the land surface to the value in the atmosphere. While the simplicity of the boundary layer methodology is convenient, it may not represent well many of the conditions found in the field. Yet, it provides an initial understanding of the weather effects on shallow subsurface conditions.

WEATHER DATA

Weather data for different locations internationally can be obtained from a number of sources, including NCAR (National Center for Atmospheric Research, Boulder, Colorado). While these weather data sets are often fairly complete, some data may be missing. For example, a typical weather data set from NCAR includes daily maximum and minimum temperature, precipitation, vapor pressure, evapotranspiration, minimum and maximum relative humidity, sea level pressure, snowfall, descriptive weather, cloud cover, wind direction, and wind speed. Radiation data (solar and long-wave) are not included in the example data set.

These data need to be processed to provide the necessary boundary conditions for TOUGH2. For example, only the minimum and maximum air temperature are often provided. A simple expression given by Fayer (2000) can be used to give time-dependent values, or

$$T_a(t_d) = T_{mean} + T_{amp}\cos[(\pi/12)(t_d - 15)] \quad (1)$$

where T_{mean} (K) and T_{amp} (K) are the average temperature and the air temperature amplitudes (i.e., the difference between the maximum and minimum temperatures), respectively, and t_d (hr) is time of day. In equation (1), the daily minimum and maximum air temperatures are assumed to occur at 3 am and 3 pm, respectively.

Other commonly missing weather data include solar and long-wave radiation. Solar radiation is the net radiation from the sun that makes it to the earth's surface. Long-wave radiation is that emitted from the atmosphere to the ground. Without plants, the radiation balance is

$$R_{solar,net} = S_t(1 - \alpha_{bg}) \quad (2)$$

$$R_{lw,net} = \varepsilon_g\left(R_{lw} - \sigma T_{surface}^4\right) \quad (3)$$

where S_t is the solar radiation (W/m^2), R_{lw} is the long-wave radiation (W/m^2), σ is the Stephan-Boltzmann constant (5.67 x 10^{-8} W/m^2-K^4), and $T_{surface}$ is the soil surface temperature. The emissivity, ε_g, and albedo, α_{bg}, of the soil are important parameters. Note that the net long-wave radiation also includes the radiation emitted by the soil surface. The net total radiation is simply the sum of the above two equations.

Solar radiation flux can be calculated using expressions given by Campbell (1985) and Fayer (2000), or

$$S_t = S_{ext}\,T_t \sin(e) \quad (4)$$

where S_t (W/m^2) is the solar radiation at the ground surface, S_{ext} (W/m^2) is the solar constant of 1367 W/m^2, and T_t is the transmission coefficient. Sin(e) refers to the sine of the solar elevation angle, or

$$\sin(e) = \sin(\phi)\sin(\delta) + \cos(\phi)\cos(\delta)\cos[(\pi/12)(t_d - t_0)] \quad (5)$$

$$\sin(\delta) = 0.39785\sin[4.869 + 0.0172J + 0.03345\sin(6.224 + 0.0172J)] \quad (6)$$

where J is the day of the year, ϕ is the latitude, δ refers to the solar declination angle, t_d (hr) is the time of day, and t_0 (hr) is the solar noon. The angles are in radians. Expressions for solar noon are given by Campbell and Norman (1998).

The transmission coefficient, T_t, is the ratio between measured to potential solar radiation, which is been calculated by the Bristow-Campbell model (Bristow and Campbell, 1984), or

$$T_t = A[1 - \exp(-B\,\Delta T^C)] \quad (7)$$

where A, B, and C are empirical constants and ΔT (^{o}C) is the daily range of air temperature (i.e., the difference between maximum and minimum temperatures). Meza and Varas (2000) have evaluated various models to estimate solar radiation from air temperature information. They showed that the Bristow and Campbell model performs well. In general, the constants A, B, and C are functions of the climate and vary from location to location. Bristow and Campbell parameters for different locales are given by the RadEst program (Donatelli, 2002). Note that the form of the Bristow-Campbell model used in RadEst is slightly different than given above.

Long-wave radiation, or radiation from the atmosphere, can be estimated from air temperature data as

$$R_{lw} = \varepsilon_a(c)\,\sigma\,T_a^4 \quad (8)$$

where ε_a(c) is the atmosphere's emissivity as a function of cloud cover, c, and T_a (K) is the air

temperature in K. The emissivity of the atmosphere including clouds is given by (Monteith and Unsworth, 1990, as discussed by Campbell and Norman, 1998)

$$\varepsilon_a(c) = (1 - 0.84c)\,\varepsilon_{ac} + 0.84c \tag{9}$$

where ε_{ac} is the clear sky emissivity, or

$$\varepsilon_{ac} = 9.2\,x10^{-6}\,T_a^2 \tag{10}$$

as given by Brutsaert (1984) and Campbell and Norman (1998) where the air temperature is in K.

The cloud cover fraction, c, can be estimated from the solar radiation transmission coefficient, T_t, through the expression (Campbell, 1985)

$$c = 2.33 - 3.33T_t \tag{11}$$

The cloud cover fraction is constrained to values between 0 and 1.0.

Wind speed is an important factor that influences the thickness of the boundary layers; where the thickness of the boundary layers is inversely proportional to the wind speed. If the wind speed increases, the boundary layer thicknesses decrease. Wind speed has important diurnal and seasonal variations in addition to changes due to weather fronts. Similarly, precipitation is very important for the saturation of the surface. No models were found to estimate wind speed or precipitation from other meteorological parameters.

A significant limitation of T2TNT, and TOUGH2, is that freezing conditions cannot be simulated. Therefore, soil temperatures below 0°C must be avoided, and snow is modeled as rain. The minimum air temperature used in simulations is 12°C in order to prevent surface temperatures below freezing.

BOUNDARY LAYER METHODOLOGY

Boundary layers occur in the atmosphere at the interface with the soil. In the case of the velocity (momentum) boundary layer, the transition is from atmospheric wind speed conditions to zero velocity at the top of the soil. There are different boundary layers for momentum (velocity), energy, and mass transfer. The evaporation boundary layer is a mass transfer boundary layer that is generally a thin (~1-10 cm) layer of air at the surface in which the water vapor concentration changes from the value at the land surface to the value in the atmosphere. The procedure to estimate the boundary layer thickness is adapted from the SiSPAT code (Braud, 1996; Braud et al., 1995) with permission.

For momentum, mass (water vapor), and heat transfer, the turbulent fluxes between the atmosphere and the soil surface are formulated in terms of resistances, or

$$\tau = \rho_a\,u^{*2} = -\rho_a\,(U_a - U_{av})/R_{aM} \tag{12a}$$
$$E = -\rho_a\,(\omega_a - \omega_{av})/R_{aV} \tag{12b}$$
$$H = -\rho_a\,c_p\,(T_a - T_{av})/R_{aH} \tag{12c}$$

where τ, E, and H are the momentum, mass (water vapor) and heat flux through the boundary layer, respectively. These formulae are appropriate when plants are included, where the "av" subscript refers to average conditions within the plant canopy, and the transfers are between the atmosphere and the canopy. In the present situation, when there is bare soil, or no plant canopy, the exchanges are between the atmosphere and the ground surface, and the "av" subscript conditions are replaced by the surface conditions.

The momentum equation is needed when a plant canopy is included to estimate the momentum distribution between the atmosphere, plant canopy, and the ground, and to calculate an average velocity in the canopy. For bare soil, the momentum equation is not needed because the surface velocity is known (equal to zero). The mass and heat flux equations are needed for a bare soil because the surface conditions are not known *a prioiri*.

Mass transfer (water vapor) and heat transfer boundary layer resistances, R_{aV} and R_{aH}, are calculated as detailed below. The boundary layer thicknesses can then be estimated. The boundary layer resistances are calculated as follows.

Wind speed and temperature profiles above the surface are assumed to be logarithmic according to

$$U_a(z_a) = \frac{u^*}{k}\left(\log\left(\frac{z_a - d}{z_{om}}\right) - \psi_m\left(\frac{z_a - d}{L}\right)\right) \tag{13a}$$

$$T_a(z_a) = \frac{\theta^*}{k}\left(\log\left(\frac{z_a - d}{z_{oh}}\right) - \psi_h\left(\frac{z_a - d}{L}\right)\right) \tag{13b}$$

where u* is the friction velocity, θ* is a characteristic temperature, d is the displacement height, z_{om} is the momentum roughness length, z_a is the elevation of the measured velocity (wind speed) and air temperature (they may be different), k is the von Karmen constant, and z_{oh} is the roughness length for heat. L is the Monin-Obukhov length given by

$$L = \frac{u^{*3}\,\overline{T}}{g\,k\left(-\frac{H}{\rho\,c_p}\right)} = \frac{u^{*3}\,\overline{T}}{g\,k\,\theta^*} \tag{14}$$

The roughness lengths are related by

$$z_{oh} = z_{om} \exp\left(-\left(2.46\,\mathrm{Re}^{*0.25} - 2\right)\right) \quad (15)$$

$$\mathrm{Re}^{*} = \frac{u^{*} z_{om}}{\nu} \quad (16)$$

The parameter d is a displacement height that is related to the height of the vegetation, while z_{om} is a roughness length for momentum that generally depends on the local terrain (see Arya, 1988). For bare soil, which is the only condition treated in the present version, d = 0., and z_{om} = 0.005 m.

The functions Ψ_m and Ψ_h in the velocity and temperature profile relationships are stability functions for the atmosphere. Typical relationships are given by

$$\psi_m(y) = 2\log(a) + \log(b) - 2\tan^{-1}(x) + \frac{\pi}{2} \qquad y<=0 \quad (17)$$

$$\psi_m(y) = -\left[0.7\,y + 0.75\left(y - \frac{5}{0.35}\right)\exp(-0.35\,y) + \frac{3.75}{0.35}\right] \qquad 0<y<=1 \quad (18)$$

$$\psi_m(y) = -5\left(1 + \log(y)\right) \qquad y>1 \quad (19)$$

$$\psi_h(y) = 2\log(b) \qquad y <=0 \quad (20)$$

$$\psi_h(y) = -\left[\left(1 + \frac{2}{3}y\right)^{1.5} + 0.667\left(y - \frac{5}{0.35}\right)\exp(-0.35\,y) + \frac{2.985}{0.35}\right] \qquad 0<y<=1 \quad (21)$$

$$\psi_h(y) = -5\left(1 + \log(y)\right) \qquad y>1 \quad (22)$$

where

$$x = (1 - 16\,y)^{1/4}$$

$$a = \frac{1+x}{2}$$

$$b = \frac{1+x^2}{2}$$

The equations for the logarithmic velocity and temperature profiles and the Monin-Obukhov length, L, are iterated upon to find the appropriate solution for the characteristic velocity, u^*, temperature, θ^*, and L. The resistance to heat is based on a combination of the turbulent flux equation, the temperature profile equation, and the Monin-Obukhov length, or

$$R_{aH} = \frac{\left(\log\left(\frac{z_a - d}{z_{oh}}\right) - \psi_h\left(\frac{z_a - d}{L}\right)\right)}{k\,u^{*}} \quad (23)$$

and the resistances for heat and mass transfer are assumed to be equal for simplicity, or

$$R_{aV} = R_{aH} \quad (24)$$

The mass transfer (water vapor) and heat transfer boundary layer thicknesses can be estimated from the resistance given above and the diffusion coefficient. For water vapor, the boundary layer thickness is given by

$$\delta_{aV} = R_{aV}\, D_V \quad (25)$$

Note that Jury et al. (1984) estimated the average evaporation boundary layer thickness using this approach as 0.5 cm.

The boundary layer thickness estimated from this procedure is only an approximation. Turbulence enhances diffusion in the outer portion of the boundary layer, so the diffusion coefficient and boundary layer thickness given by equation 25 can be thought of as a minimum value. Based on velocity profiles for air flowing over a flat plate (White, 1974), the total boundary layer thickness may be up to a factor of 10 times the value estimated in equation 25. Note that the change in water vapor concentration is not linear in the boundary layer; it changes much more quickly nearer the soil surface than further out in the boundary layer.

EXAMPLE

An example of weather data and the variation in the calculated boundary layer thickness are presented in this section. As mentioned earlier, weather data from Ft. Leonard Wood, Missouri, were used. Ft. Leonard Wood is the site of a landmine field test facility as modeled by Phelan and Webb (2003). For reference, the total annual precipitation is about 80 cm.

Figures 2a and 2b show the effect of rainfall on the surface saturation. The precipitation variation is shown in Figure 2a. There are two discrete rainfall events. The resulting surface saturation is shown in Figure 2b. Before the rain, the calculated surface saturation was about 0.02. Immediately after the first rainfall event during Day 206, the surface saturation increases to 0.3 and then quickly returns to its previous value. For the rainfall event during Day 210 to 211, the surface saturation increases to a maximum of slightly over 50%. After the rainfall event, the surface saturation returns to its previous value.

Figures 3a and 3b show the diurnal variation of radiation and the soil surface temperature. Figure 3a shows the variation in solar (blue), long-wave (red), and net (yellow) radiation during this same time period as well as the surface temperature variation. The solar radiation has a strong diurnal variation as expected. The long-wave radiation is essentially constant because the air temperature does not vary significantly. The net radiation is strongly positive during the day due to the solar component. At night, the net radiation is approximately zero or slightly

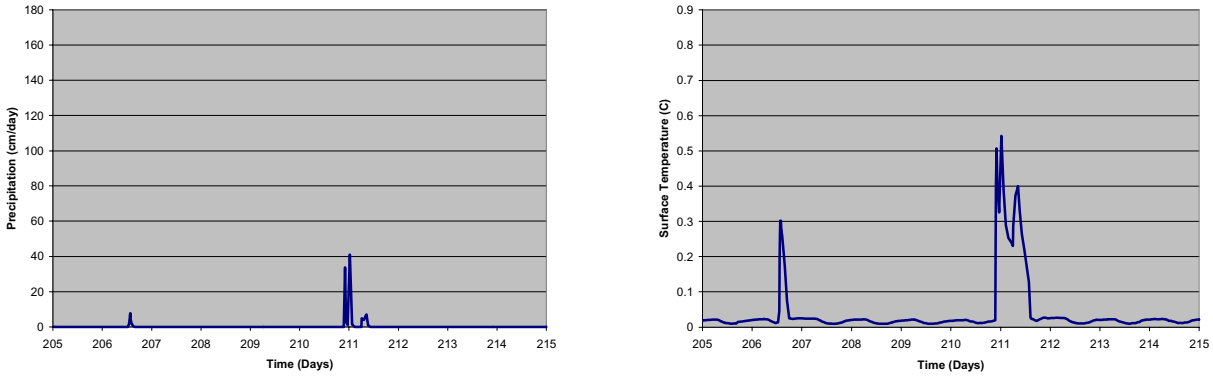

(a) *(b)*

Figure 2. Precipitation and Soil Surface Saturation

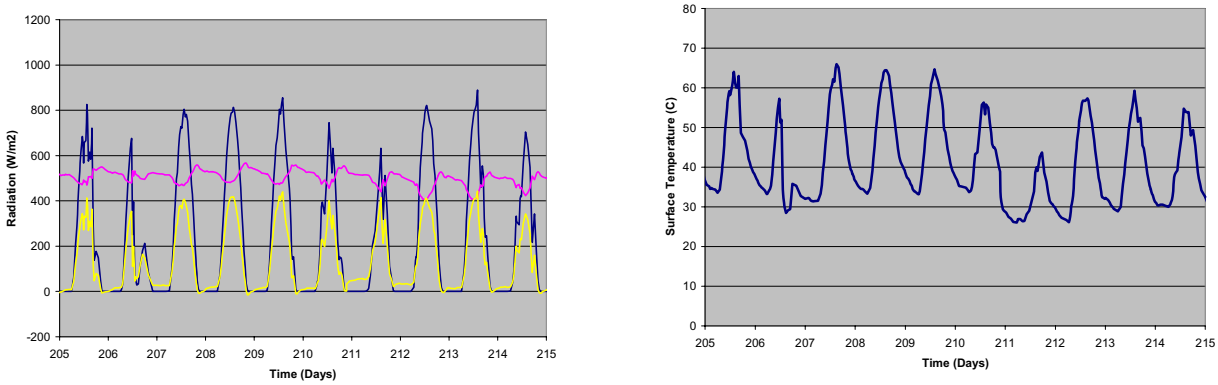

(a) *(b)*

Figure 3. Radiation Balance and Soil Surface Temperature

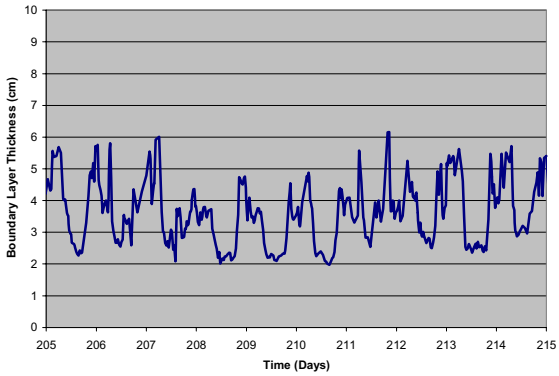

Figure 4. Calculated Boundary Layer Thickness

negative. The resulting surface temperature variation shown in Figure 3b also shows a strong diurnal variation, varying from 25 to 30°C at night to a maximum of about 65°C during the day.

Figure 4 shows the variation in the calculated boundary layer thickness during this period, where the value is 10 times equation (25) as discussed above. The boundary layer thickness varies by a factor of 2 to 3 in a single day. Assuming a constant boundary layer thickness is obviously not appropriate due to the strong variation.

CONCLUSIONS

Implementation of land surface boundary conditions, including the weather and boundary layer model, has been discussed for a variation of the TOUGH2 code called T2TNT. Significant diurnal variations of surface soil saturation and temperature are caused by precipitation and solar radiation. The calculated boundary layer thickness also varies significantly during the day. Therefore, assuming constant boundary conditions for the land surface is not appropriate for near-surface calculations.

ACKNOWLEDGMENTS

The work was sponsored by the Geneva International Center for Humanitarian Demining (GICHD) under the direction of Havard Bach. Sandia is a multiprogram laboratory operated by Sandia Corporation, a Lockheed Martin Company, for the United States Department of Energy under Contract DE-AC04-94AL85000.

NOMENCLATURE

c	cloud cover fraction
c_p	specific heat
d	displacement height
D	diffusivity
E	evaporation mass flux
g	gravity
H	heat flux
k	von Karmen constant (=0.4)
L	Monin-Obukhov length
R	resistance
T	temperature
T_t	transmission coefficient
$\overline{T}$	average temperature between z_a and z_{av}
u*	friction velocity
U	velocity
z	elevation above ground surface
z_{oh}	roughness length for heat
z_{om}	roughness length for momentum
ρ	density
δ	boundary layer thickness
τ	momentum flux
ω	mass fraction
Ψ_m	velocity profile function
Ψ_h	temperature profile function
Θ*	characteristic temperature

Subscripts

a	air
av	average
aH	heat
aM	momentum
aV	water vapor
v	vapor

REFERENCES

Arya, S.P., 1988, *Introduction to Micrometeorology*, Academic Press, San Diego.

Braud, I., Dantas-Antonio, A.C., Vauclin, M., Thony, J.L., and Ruelle, P., 1995, "A Simple Soil-Plant-Atmosphere Transfer model (SiSPAT): development and field verification," *J. Hydrol*., 166:213-250.

Braud, I., 1996, SiSPAT User's Manual, Version 2.0, LTHE, October 1996, 83 pp. (available from LTHE, B.P. 53, 38041 Grenoble, Cedex 0, France)

Bristow, K., and Campbell, G., 1984, "On the relationship between incoming solar radiation and daily minimum and maximum temperature, *Agric. For. Meteorol*., 31:159-166.

Brutsaert, W., 1984, *Evaporation into the Atmosphere: Theory, History, and Applications,* D. Reidel, Boston.

Campbell, G.S., 1985, *Soil Physics with Basic: Transport Models for Soil-Plant Systems*, Elsevier, Amsterdam.

Campbell, G.S., and Norman, J.M., 1998, *An Introduction to Environmental Biophysics,* 2nd Edition, Springer, New York.

Donatelli, M., 2002, RadEst Version 3.00, http:/www.isci.it/tools.

Fayer, M.J., 2000, UNSAT-H Version 3.0: Unsaturated Soil Water and Heat Flow Model Theory, User Manual, and Examples, PNNL-13249, Pacific Northwest National Laboratory, Richland, Washington.

Jury, W.A., Spencer, W.F., and Farmer, W.J., 1984, "Behavior Assessment Model for Trace Organics in Soil: IV. Review of Experimental Evidence," *J. Environ. Qual*, 13:580-586.

Meza, F., and Varas, E., 2000, "Estimation of mean monthly solar global radiation as a function of temperature," *Agric.l For. Meteorol.*, 100:231-241.

Monteith, J.L., and Unsworth, M.H., 1990, *Principles of Environmental Physics,* 2nd Edition, Edward Arnold, London.

Phelan, J.M., and Webb, S.W., 2003, "Data-Model Comparison of Field Landmine Soil Chemical Signatures at Ft. Leonard Wood", SPIE Proceedings, Orlando.

Webb, S.W., and Phelan, J.M., 2000, "Effect of Diurnal and Seasonal Weather Variations on the Chemical Signatures from Buried Landmines/UXO," in *Detection and Remediation Technologies for Mines and Minelike Targets V*, A.C. Dubey, J.F. Harvey, J.T. Broach, R.E. Dugan, eds, Proceedings of SPIE.

Webb, S.W., and Phelan, J.M., 2002, Effect of Weather on the Predicted PMN Landmine Chemical Signature for Kabul, Afghanistan, SAND2002-3779, Sandia National Laboratories, Albuquerque, NM.

Webb, S.W., and Phelan, J.M., 2003, "Effect of Weather on Landmine Chemical Signatures for Different Climates," Proceedings of SPIE, Orlando, FL.

Webb, S.W., Finsterle, S.A., Pruess, K., and Phelan, J.M., 1998, "Prediction of the TNT Signature from Buried Landmines," *TOUGH Workshop '98*.

Webb, S.W., Pruess, K., Phelan, J.M., Finsterle, S.A., 1999, "Development of a Mechanistic Model for the Movement of Chemical Signatures From Buried Landmines/UXO," in *Detection and Remediation Technologies for Mines and Minelike Targets IV*, A.C. Dubey, J.F. Harvey, J.T. Broach, R.E. Dugan, eds, Proceedings of SPIE, Vol. 3710, pp. 270-282.

White, F.M., 1974, *Viscous Fluid Flow,* McGraw-Hill, New York.